Anisotropic surface-state-mediated RKKY interaction between adatoms

Paul N. Patrone[1,2,3,*] and T. L. Einstein[1,†]

[1]*Department of Physics, University of Maryland, College Park, Maryland 20742-4111, USA*

[2]*Institute for Research in Electronics and Applied Physics, University of Maryland, College Park, Maryland 20742, USA*

[3]*Center for Nanoscale Science and Technology, National Institute of Standards and Technology, Gaithersburg, Maryland 20899, USA*

(Received 13 September 2011; revised manuscript received 17 December 2011; published 18 January 2012; corrected 24 January 2012)

Motivated by recent numerical studies of Ag on Pt(111), we derive an expression for the RKKY interaction mediated by surface states, considering the effect of anisotropy in the Fermi edge. Our analysis is based on a stationary phase approximation. The main contribution to the interaction comes from electrons whose Fermi velocity $\mathbf{v}_F$ is parallel to the vector $\mathbf{R}$ connecting the interacting adatoms; we show that, in general, the corresponding Fermi wave vector $\mathbf{k}_F$ is not parallel to $\mathbf{R}$. The interaction is oscillatory; the amplitude and wavelength of oscillations have angular dependence arising from the anisotropy of the surface-state band structure. The wavelength, in particular, is determined by the projection of this $\mathbf{k}_F$ (corresponding to $\mathbf{v}_F$) onto the direction of $\mathbf{R}$. Our analysis is easily generalized to other systems. For Ag on Pt(111), our results indicate that the RKKY interaction between pairs of adatoms should be nearly isotropic and so cannot account for the anisotropy found in the studies motivating our work. However, for metals with surface-state dispersions similar to Be(10$\bar{1}$0), we show that the RKKY interaction should have considerable anisotropy.

DOI: 10.1103/PhysRevB.85.045429 PACS number(s): 73.20.At, 68.35.Md, 73.90.+f

I. INTRODUCTION

Surface reconstruction and self-assembly at interfaces have attracted considerable interest due to the desire to tailor electronic and other properties of semiconductor devices. Understanding the dominant interactions between atoms on surfaces is crucial for describing these larger-scale reconstruction processes. Classical models of surface stress, such as the Frenkel-Kontorova model,[1,2] have been successful in describing many experimental systems.[3–6] However, recent work suggests that classical theories are unable to predict the formation of structures on certain heteroepitaxial systems. By comparing numerical results to experimental data, Stepanyuk *et al.* showed how quantum-mechanical interactions could lead to the self-assembly of one-dimensional Co chains and Fe superlattices on Cu(111).[7,8] More recently, Refs. 9 and 10 used density functional theory (DFT) and kinetic Monte Carlo simulations to show that *anisotropy* in the quantum-mechanical interactions between adsorbed atoms (adatoms) is crucial for the formation of striped dislocation patterns seen when Ag is deposited on Pt(111).[11]

Motivated by these works, our primary goal in this paper is to derive an analytic expression for the *anisotropic* surface-state[12,13] (SS) mediated Ruderman-Kittel-Kasuya-Yosida (RKKY) interaction[14–17] between adatoms on an fcc surface. While perturbative calculations of the RKKY interaction have been performed in two dimensions by Lau and Kohn[18] and others,[19] we emphasize that, to the best of our knowledge, these previous studies only considered isotropic band structures.[20–22] Our analysis, however, specifically accounts for the anisotropy in the interaction, which is induced by a more realistic SS band. In this paper, we focus our analysis primarily on the the (111) surface of an fcc crystal so that, as a secondary goal, we may compare our results with Refs. 7–10. However, the techniques we employ are easily generalized to other lattice geometries and systems; we will show, for example, how our main result can be used to describe the RKKY interaction on surfaces such as Be(10$\bar{1}$0) and Cu(110), which both have a highly anisotropic surface-state band.[23]

In Ref. 24, one of us proposed that the main contribution to the RKKY interaction comes from electrons whose Fermi velocity (rather than Fermi wave vector) is parallel to the vector separating the adatoms. A version of this idea was, in fact, shown earlier by Roth *et al.*,[25,26] whose analysis we extend to surfaces and two-dimensional (2D) systems. Our main analytical tool will be a stationary phase approximation of the relevant, oscillatory integrals. This technique has the benefit of revealing the essential physics of the RKKY interaction, at the cost of limiting our result to the far-field regime; we provide a criterion that indicates when our result is valid. The generality of our approach is closely related to the stationary phase approximation and stems from the fact that, in the far-field limit, the interaction is determined by the local structure of the Fermi edge (i.e., a few electron states); thus, one need not perform complicated integrals over all surface states.

We find that the 2D RKKY interaction is oscillatory and bounded by an envelope that decays as inverse distance squared, in agreement with experimental and numerical studies.[7,8,18–21] For a (111) fcc surface, our analysis predicts a sixfold anisotropy in the interaction; however, we find less variation in the interaction wavelength than in Ref. 9. Below we indicate conceptual differences between our approach and those of the aforementioned references.

The remainder of the paper is organized as follows. In Sec. II, we evaluate an analytical formula for the anisotropic, RKKY interaction in two dimensions. In Sec. III A we discuss the essential physics of the interaction and give a criterion that indicates when our main result is valid. In Sec. III B we briefly review experimental evidence of the 2D RKKY interaction, while in Sec. III C we discuss our main result in the context of Ag on Pt(111) (Refs. 9 and 10). In Sec. III D 1 we highlight the key quantities needed to determine the RKKY interaction for different lattice geometries, and in Sec. III D 2 we consider complications that arise in metals such as Be(10$\bar{1}$0), i.e., when

the SS band is centered at special points on the boundary of the surface Brillouin zone. Section III E compares our work with other analytical treatments of the RKKY interaction, and Sec. III F discusses complications beyond the scope of our work. Section III G explores open questions and extensions of our analysis. Section IV restates our main conclusions.

II. 2D ANISOTROPIC RKKY INTERACTION

It is well known that the {111} surfaces of each noble metal possess a partially filled, "metallic" *sp* Shockley surface state (with its minimum at the zone center $\overline{\Gamma}$),[27] which can mediate interactions between adatoms.[28,29] The general form of the corresponding 2D RKKY interaction is[25]

$$\Delta = -\mathcal{P}\int d^2\mathbf{k} d^2\mathbf{k}' \, \frac{e^{-i(\mathbf{k}-\mathbf{k}')\cdot\mathbf{R}}|J_{\mathbf{k}\mathbf{k}'}|^2}{E_{\mathbf{k}'}-E_{\mathbf{k}}} f(E_{\mathbf{k}})[1-f(E_{\mathbf{k}'})], \quad (1)$$

where $\mathcal{P}$ indicates that the integral should be interpreted as a principal value. The vector $\mathbf{R}$ connects the positions of the interacting adatoms. The Fermi function is denoted by $f(E_k)$, and E_k is the energy of a SS with the wave vector $\mathbf{k}$. When multiplied by $f(E_{\mathbf{k}})[1-f(E_{\mathbf{k}'})]$, the exchange integral $J_{\mathbf{k}\mathbf{k}'}$ describes a coupling event whereby a SS below the Fermi energy is upscattered to a state above the Fermi energy via an interaction with an adatom; the conjugate transpose $J^{\dagger}_{\mathbf{k}\mathbf{k}'}$ describes the opposite process in which the upscattered SS returns to its original state. The presence of $\exp[-i(\mathbf{k}-\mathbf{k}')\cdot\mathbf{R}]$ reveals that the interaction is mediated by a weighted sum of symmetric and antisymmetric surface states. Here we refer specifically to the symmetry of $\cos[(\mathbf{k}-\mathbf{k}')\cdot\mathbf{R}]$ under the reflections about the midpoint of $\mathbf{R}$ [cf. Eq. (4) for motivation]. Integration runs over all $\mathbf{k}$ in the first Brillouin zone of a single band; we neglect contributions from other bands.

We assume that the coupling between a SS and an adatom is the same at both adatom locations; consequently, $\mathbf{R}$ is a Bravais lattice vector. This is a reasonable assumption since the adatoms typically adsorb at energetically favored high-symmetry sites [atop, bridge, or center (hollow), depending on the adatom and substrate]. In such cases, adatom pairs will be *separated* by 2D Bravais lattice vectors, regardless of their registry with the substrate. The 2D SS wave vectors $\mathbf{k}$ and $\mathbf{k}'$, which mediate the interaction, can be regarded as free-electron-like states for the case of the metallic Shockley state but in general must be treated as Bloch states (cf. Sec. III D 2).

For simplicity, we assume that one *s* orbital from each substrate atom contributes to the SS conduction band; we calculate the conduction band using a nearest-neighbor, tight-binding approximation, which provides a semiquantitative approximation for the metallic surface state on Cu(111).[29,30] For the (111) face of an fcc crystal,

$$E(\mathbf{k}) = \epsilon\left[3-\cos\left(\frac{2}{\sqrt{3}}\mathbf{k}\cdot\mathbf{a}_{\parallel}\right)-\cos(k_+)-\cos(k_-)\right], \quad (2)$$

where $\mathbf{k} = (k_x,k_y)/a$, $k_\pm = (\mathbf{k}\cdot\mathbf{a}_\perp) \pm (1/\sqrt{3})(\mathbf{k}\cdot\mathbf{a}_\parallel)$, $\mathbf{a}_\parallel = a(\sin(\theta),\cos(\theta))$, and $\mathbf{a}_\perp = a(\cos(\theta),-\sin(\theta))$. The constant a is the interatomic spacing of the substrate atoms (k_x and k_y are dimensionless), and ϵ is a parameter having units of energy. When the crystal axes are held fixed, $-\theta$ is the angular coordinate of $\mathbf{R}$.

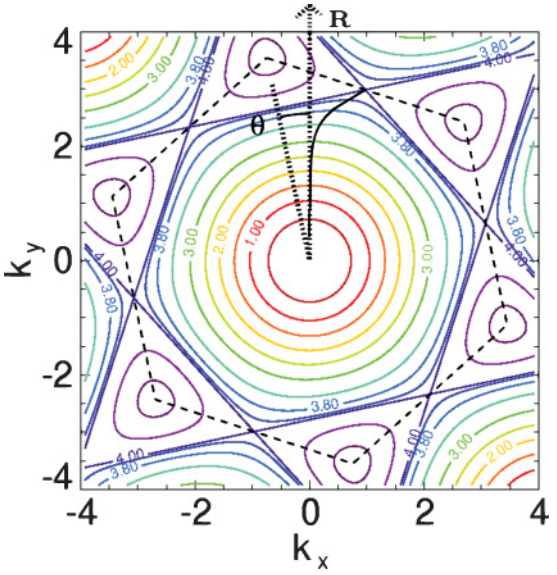

FIG. 1. (Color online) Constant-energy curves [via Eq. (2)] for E/ϵ when $\theta = \pi/15$. The vertical dotted line points in the k_y direction and is parallel to $\mathbf{R}$. The slanted dotted line shows the angle through which the constant-energy curves have been rotated. The black dashed contour is the boundary of the first Brillouin zone. The solid black curve connecting the origin to the $E/\epsilon = 4$ contour intersects the point on each constant-energy contour for which k_y is maximized, so that $dk_y/dk_x = 0$ (which is the stationary phase condition for the dk_x integration). The intersection of this curve and the Fermi edge marks the location of the surface states that dominate the RKKY interaction. The solid black curve was found by numerically solving Eqs. (2) and (11) as a function of E/ϵ.

Concerning the rotation angle, however, we adopt the alternate perspective that $\mathbf{R}$ is always fixed in the $\hat{\mathbf{y}}$ direction, so that the crystal axes are rotated by θ (cf. Fig. 1): $\mathbf{R} = R\,\hat{\mathbf{y}}$. We make this choice to clarify the analysis; specifically, we anticipate[24] that the dominant contribution to the interaction comes from electrons whose Fermi velocity is parallel to $\mathbf{R}$. By applying a stationary phase approximation to Eq. (1), we will show that this idea arises naturally in the rotated frame.

By inversion symmetry, we may replace $1-f(E_{k'})$ by 1, as this does not change the principal value expressed by Eq. (1).[25] We may also simplify Eq. (1) by applying the substitution $\boldsymbol{k}(\boldsymbol{k}') \to -\boldsymbol{k}(-\boldsymbol{k}')$ to all $\boldsymbol{k}(\boldsymbol{k}')$ for which $k_y(k'_y) < 0$.[31] Changing variables from $k_y(k'_y)$ to $E(E')$ then yields

$$\Delta = \mathcal{P}\int_0^{E_{\max}} dE \int_0^{E_{\max}} dE' \int dk_x \int dk'_x \, \frac{f(E)\,|J_{\mathbf{k}\mathbf{k}'}|^2}{E-E'} \times \mathcal{V}_y^{-1}(E,k_x)\mathcal{V}_y^{-1}(E',k'_x)P(k_y,k'_y), \quad (3)$$

$$P(k_y,k'_y) = [e^{-i(k_y-k'_y)R} + e^{-i(k_y+k'_y)R} + \text{c.c.}], \quad (4)$$

where c.c. stands for complex conjugate and $\mathcal{V}_y^{-1}(E,k_x) = \partial k_y/\partial E$. The product $a\mathcal{V}_y(E)/\hbar$ is the k_y component of the group velocity of a wave packet centered about $\hbar\mathbf{k}$.[32] Note that $k_y = k_y(k_x,E)$.

In the limit of large R (we specify this condition more precisely below), the integrand in Eq. (3) oscillates rapidly when $k_y(k_x,E)$ changes as a function of only k_x, keeping E fixed. We expect cancellation of the integrand due to

destructive interference, except when $\partial k_y/\partial k_x|_E = 0$, when k_y is a maximum on each constant-energy curve (cf. Fig. 1).[25,33,34] These extrema correspond to a SS whose group velocity is parallel to $\mathbf{R}$.

Thus, fix E and expand k_y about its maximum; namely,

$$k_y(E,k_x) \approx k_y(E,\check{k}_{x,E}) - (k_x - \check{k}_{x,E})^2/\mathfrak{n}(E), \quad (5)$$

$$1/\mathfrak{n}(E) = -\tfrac{1}{2}\partial^2 k_y(E,k_x)/\partial k_x^2\,\big|_{k_x=\check{k}_{x,E}}, \quad (6)$$

where $\check{k}_{x,E}$ maximizes $k_y(E,k_x)$ for a given E. Equation (5) states that for each E, there is a group of k states centered around $(\check{k}_x,k_y(E,\check{k}_x))$ mediating the interaction in a *coherent* manner. The function $\mathfrak{n}(E)$ measures the approximate number of k states that contribute to the interaction for a given E. We will show later how Eqs. (3), (5), and (6) provide a more precise definition of the far-field limit.

We substitute Eq. (5) into Eq. (3) and extend the integration in k_x,k_x' from $-\infty$ to ∞. Approximating $J_{\mathbf{k}\mathbf{k}'} \approx J_{\mathbf{k}\mathbf{k}'}|_{k_x=\check{k}_{x,E},\,k_x'=\check{k}_{x,E}'} = J_{EE'}$ and $\mathcal{V}_y(E,k_x) \approx \mathcal{V}_y(E,\check{k}_{x,E})$ yields

$$\Delta = \frac{\pi}{R}\int_0^{E_{\max}} dE \int_0^{E_{\max}} dE' \, \frac{|J_{EE'}|^2[f(E)-f(E')]\sqrt{\mathfrak{n}(E)\mathfrak{n}(E')}}{2[E-E']\mathcal{V}_y(E,\check{k}_{x,E})\mathcal{V}_y(E',\check{k}'_{x,E})} \times \{\exp[i(\check{k}_y-\check{k}'_y)R] + i\exp[i(\check{k}_y+\check{k}'_y)R] + \text{c.c.}\}. \quad (7)$$

The substitution $f(E) \to [f(E) - f(E')]/2$ is valid by inversion symmetry;[25] that is, switching E and E' in Eq. (3) is equivalent to multiplying the expression by -1. This substitution eliminates the pole along the real E axis, so that Eq. (7) is the principal value of Eq. (3).

In the spirit of Ref. 25, we assume that the major contribution to Eq. (7) comes from the Fermi energy ϵ_F. We make the substitution $E = E' = \epsilon_F$ and approximate $k_y|_{k_x=\check{k}_{x,F}} \approx \check{k}_{y,F} + \mathcal{V}_F^{-1}(E-\epsilon_F)$, neglecting terms $\mathcal{O}[(E-\epsilon_F)^2]$.[35] The vector $\check{\mathbf{k}}_F = (\check{k}_{x,F},\check{k}_{y,F})$ points to the maximum of the Fermi edge in the rotated reference frame, and $\mathcal{V}_F = \mathcal{V}_y(\epsilon_F,\check{k}_{x,F})$ is proportional to the Fermi velocity v_F via $\mathcal{V}_F = \hbar v_F/a$. Hereafter, for brevity, we refer to $\check{k}_{y,F}$ as k_s; the subscript s is intended to remind the reader that $2\check{\mathbf{k}}_F$ spans the Fermi edge.

When the limits of integration are extended to $\pm\infty$,[33] Eq. (7) simplifies to

$$\Delta = \frac{\pi|J_{\epsilon_F,\epsilon_F}|^2\mathfrak{n}(\epsilon_F)}{2\mathcal{V}_F^2 R}\int_{-\infty}^{\infty} dE\int_{-\infty}^{\infty} dE' \, \frac{f(E)-f(E')}{E-E'} \times \left[e^{i\mathcal{V}_F^{-1}[E-E']R} - i\,e^{i[2k_s+\mathcal{V}_F^{-1}(E+E'-2\epsilon_F)]R} + \text{c.c.}\right]. \quad (8)$$

Equation (8) can be evaluated by the residue theorem. By definition, $f(E) = \{\exp[(E-\mu)/\tau]+1\}^{-1} \approx \{\exp[(E-\epsilon_F)/\tau]+1\}^{-1}$ (μ is the chemical potential, and $\tau = k_B T$ is Boltzmann's constant times the temperature); the Fermi function has poles at $E = \epsilon_F \pm (2n+1)\pi i\tau, n = 0,1,2\ldots$ Carrying out the two integrations yields an odd-power geometric series, which reduces to

$$\Delta = -2\pi^3\tau\frac{|J_{\epsilon_F,\epsilon_F}|^2\mathfrak{n}(\epsilon_F)}{\mathcal{V}_F^2}\frac{\sin(2k_sR)}{\sinh[2\pi\tau R/\mathcal{V}_F]R} \quad (9a)$$

$$\to [\tau\to 0] \; -\pi^2\frac{|J_{\epsilon_F,\epsilon_F}|^2\mathfrak{n}(\epsilon_F)}{\mathcal{V}_F}\frac{\sin(2k_sR)}{R^2}. \quad (9b)$$

We emphasize that the wavelength of this oscillatory expression is π/k_s, where $k_s = \check{k}_{y,F}$ is the projection onto the unit vector $\hat{\mathbf{R}}$ of the Fermi wave vector whose velocity is parallel to $\mathbf{R}$; i.e., it is $\pi R/(\check{\mathbf{k}}_F\cdot\mathbf{R})$. We treat $J_{\epsilon_F,\epsilon_F}$ as a free parameter; strictly speaking then, Eq. (9) is well defined only for $\mathbf{R}$, a Bravais lattice vector. This becomes important when the surface state does not have simple 2D free-electron behavior (cf. Sec. III D 2). The factor of τ appearing in the coefficient of (9) comes from the ratio E/τ in the chemical potential.

To complete the analysis, we must compute $\mathcal{V}_y(E,k_x)$, k_s, and $\mathfrak{n}(E)$. Implicit differentiation of Eq. (2) with respect to k_y, keeping k_x fixed, gives $\mathcal{V}_y(E,k_x)$;

$$\mathcal{V}_y(E,k_x) = \left.\frac{\partial E}{\partial k_y}\right|_{k_x} = a\epsilon\left[\frac{2}{\sqrt{3}}\cos(\theta)\sin\left(\frac{2}{\sqrt{3}}\mathbf{k}\cdot\mathbf{a}_\parallel\right) - (\mathbf{p}\cdot\mathbf{a}_\parallel)\sin(k_-) - (\mathbf{q}\cdot\mathbf{a}_\parallel)\sin(k_+)\right], \quad (10)$$

where $\mathbf{p} = a^{-1}(1,1/\sqrt{3}), \mathbf{q} = a^{-1}(1,-1/\sqrt{3})$. To find $\check{k}_y(E)$, differentiate Eq. (2) with respect to k_x for fixed E, which gives

$$0 = \frac{\partial k_y}{\partial k_x} = \frac{2}{\sqrt{3}}\sin(\theta)\sin\left(\frac{2}{\sqrt{3}}\mathbf{k}\cdot\mathbf{a}_\parallel\right) + (\mathbf{p}\cdot\mathbf{a}_\perp)\sin(k_-) + (\mathbf{q}\cdot\mathbf{a}_\perp)\sin(k_+). \quad (11)$$

Solving Eqs. (2) and (11) simultaneously yields $\check{k}_y(E)$ and $\check{k}_x(E)$. Equation (6) defines $\mathfrak{n}(E)$; using Eq. (11) and $\partial k_y/\partial k_x|_{k_x=\check{k}_{x,E}} = 0$, one finds

$$\mathfrak{n}(E)^{-1} = \frac{1}{2}\left\{\frac{4}{3}\sin^2(\theta)\cos\left(\frac{2}{\sqrt{3}}\check{\mathbf{k}}\cdot\mathbf{a}_\parallel\right) + (\mathbf{p}\cdot\mathbf{a}_\perp)^2\cos(\check{k}_-) + (\mathbf{q}\cdot\mathbf{a}_\perp)^2\cos(\check{k}_+)\right\} \Big/ \left\{\frac{2}{\sqrt{3}}\cos(\theta)\sin\left(\frac{2}{\sqrt{3}}\check{\mathbf{k}}\cdot\mathbf{a}_\parallel\right) - (\mathbf{p}\cdot\mathbf{a}_\parallel)\sin(\check{k}_-) - (\mathbf{q}\cdot\mathbf{a}_\parallel)\sin(\check{k}_+)\right\}, \quad (12)$$

where $\check{\mathbf{k}} = (\check{k}_x,\check{k}_y)$ and $\check{k}_\pm = k_\pm(\check{k}_x,\check{k}_y)$.

III. DISCUSSION

A. Elements of the 2D RKKY interaction for a (111) fcc surface

Equations (2) and (9)–(12) completely describe the RKKY interaction for a (111) fcc surface. The essential physics, however, is manifest in Eq. (9). Specifically, (i) the interaction becomes stronger as more SS contribute [$\mathfrak{n}(\epsilon_F)$ increases] and/or the coupling between a SS and an adatom becomes stronger ($|J_{\epsilon_F,\epsilon_F}|^2$ increases), (ii) the interaction amplitude *decreases* as the SS Fermi velocity increases ($\mathcal{V}_F$ increases), and (iii) the interaction oscillates with a periodicity determined by $2k_s$, twice the k_y component of the Fermi wave vector corresponding to the Fermi velocity that is parallel to $\mathbf{R}$. The oscillations arise from the symmetry (with respect to $\mathbf{R}$) of the SS mediating the interaction.

When $\tau \to 0$, Eq. (9) decays as $1/R^2$. The low-temperature limit is defined by estimating $\mathcal{V}_F = \mathcal{O}(\hbar^2 k_F/a\,m_{\text{eff}})$, where k_F and m_{eff} are the Fermi wave vector and effective mass of the SS. For Ag(111), Table 1 of Ref. 20 gives experimental values of these quantities; one finds that $\mathcal{V}_F = \mathcal{O}(1\text{eV})$, so that Eq. (9) decays as $1/R^2$ whenever $R\tau \ll 1$ eV. At room temperature ($\tau = 1/40$ eV), for example, we estimate that

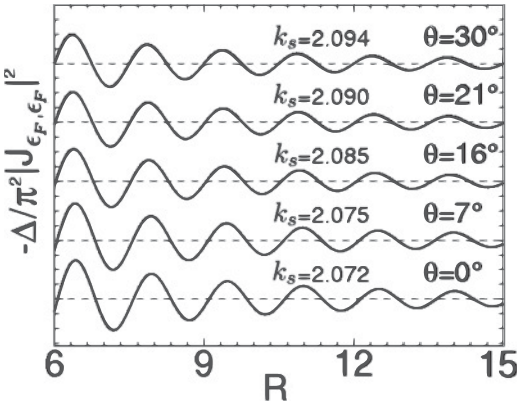

FIG. 2. RKKY interaction $-\Delta/(\pi^2|J_{\epsilon_F,\epsilon_F}|^2)$ [Eq. (9)] on a (111) fcc surface as a function of R (in units of $a = 0.289$ nm for Ag and $a = 0.256$ nm for Cu) at zero temperature when $\epsilon_F/\epsilon = 3$. Values of θ are approximately the angles an adatom makes with its second, ninth, seventh, fourteenth, and first nearest neighbors, from bottom to top. All curves oscillate about zero, indicated for each curve by a dashed line; these lines are separated by intervals of 0.1 along the vertical axis. Values of k_s are in units of a^{-1}.

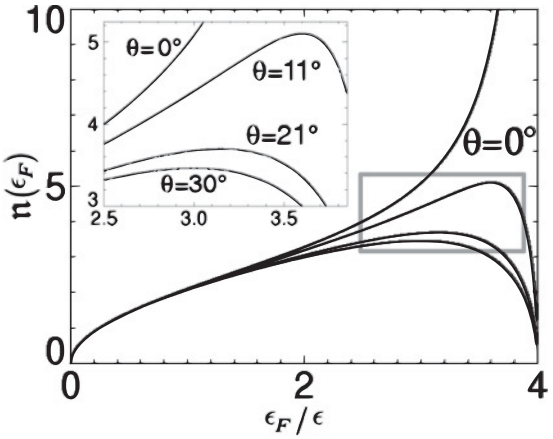

FIG. 3. The function $\mathfrak{n}(\epsilon_F)$ of the constant energy contour maxima for different angles [cf. Eqs. (5), (6), and (12)]. Note that for $\theta = 0$ the amplitude diverges when $\epsilon_F/\epsilon \to 4$, so that Eq. (5) overestimates the number of surface states contributing to the interaction. For all other values of θ, $\mathfrak{n}(\epsilon_F) \to 0$ when $\epsilon_F/\epsilon \to 4$ since the maximum of the constant energy curves becomes infinitely sharp in this limit. The far-field regime in which Eq. (9) is valid is given by $R/\mathfrak{n}(\epsilon_F) \gg 1$.

such an exponential decay in Eq. (9) only becomes appreciable when $Ra \gtrsim 10a$ for this system (recall that a is the interatomic distance).

Equation (9) differs in several respects from its 3D counterpart. In the *bulk* of a crystal, the RKKY interaction falls off as $1/R^3$ when $\tau = 0$ due to the increased dimensionality of the lattice.[25] Also, in 3D the number of electrons contributing to the interaction is proportional to $\mathfrak{n}(\epsilon_F)^2$ since the dominant electrons live on a Fermi *surface* (as opposed to an edge).

Numerically solving the system of Eqs. (2) and (11) for $\check{\boldsymbol{k}}$ reveals that $\check{k}_y$ is a function of θ (cf. Figs. 1 and 2). This implies that anisotropy in the SS band structure induces anisotropy in both the amplitude [via $\mathcal{V}_F$ and $\mathfrak{n}(\epsilon_F)$] and the periodicity of the interaction (cf. Fig. 2). From the structure of the lattice, we find (i) that the anisotropy is sixfold and (ii) that the interaction amplitude is strongest for $\theta = 0, \pi/3, 2\pi/3, \ldots$, i.e., when $\mathbf{R}$ is perpendicular to the flattest part of the Fermi edge (cf. Figs. 1–3).

Inspection of Fig. 1, however, reveals that the SS band structure is nearly isotropic when $E/\epsilon \lesssim 3$. This observation is confirmed by expanding Eq. (2) for small $\mathbf{k}$:

$$\frac{E(\mathbf{k})}{\epsilon} \approx (a|\mathbf{k}|)^2 - \frac{(a|\mathbf{k}|)^4}{12} + \frac{[10+\cos(6\theta)](a|\mathbf{k}|)^6}{3240}. \qquad (13)$$

The dispersion relation is isotropic up through $\mathcal{O}(|\mathbf{k}|^4)$. When the Fermi energy $\epsilon_F/\epsilon \lesssim 3$, the component $\check{k}_{x,F} \approx 0$ and $ak_s \approx 6^{1/2}[1+\sqrt{1-(\epsilon_F/3\epsilon)}]^{1/2}$. In this limit, the interaction given by Eq. (9) is approximately independent of θ (cf. Fig. 2). Anisotropy in the interaction becomes apparent only when $\epsilon_F/\epsilon \gtrsim 3$.

We identify the far-field regime by determining the minimum values of R for which our model is valid. Returning to Eqs. (3) and (7), when $R/n(\epsilon_F) \ll 1$, extending the limits of integration of k_x, k_x' to infinity grossly overestimates the number of k states contributing to the interaction. In particular, for $E/\epsilon_F = 4$ and $\theta = 0$, the amplitude of the interaction diverges, which indicates a total failure of the approximation for all R at this angle. Hence, Eq. (9) is valid, provided that not too many k states contribute to the interaction; namely, $R/\mathfrak{n}(\epsilon_F) \gg 1$ (cf. Fig. 3). When the opposite limit holds $[R/\mathfrak{n}(\epsilon_F) \ll 1]$, Eq. (9) can be corrected by not extending the limits of integration of k_x, k_x' to $\pm\infty$ in Eq. (3); e.g., for $\theta = 0$ and $\epsilon_F/\epsilon = 4$, a suitable range of integration in k_x, k_x' would be $[-\pi/2, \pi/2]$, which corresponds to the length of a side of the $E/\epsilon = 4$ constant-energy curve in Fig. 1.

B. Experimental evidence of isotropic 2D RKKY interactions

At low temperatures, scanning tunneling microscopy (STM) measurements of Co adatoms on Cu(111) are capable of directly imaging standing waves in the electronic density of states (DOS).[7] By comparing such experiments with DFT calculations [based on the Korringa-Kohn-Rostoker (KKR) Green's function method] of the SS-mediated interaction, Stepanyuk *et al.*[7] showed that the envelope bounding oscillations in the interaction energy falls off as $1/R^2$ for distances larger than roughly ten atomic spacings.[36] In the far-field limit, this implied that (i) the interaction is dominated by the SS and (ii) bulk electronic states do not contribute to the $\mathbf{R}$ dependence of the coupling between adatoms. Stepanyuk *et al.* also found that the interaction wavelength is π/k_F at large distances. At short and intermediate distances (corresponding to $R \lesssim 10$ in our model), they found that screening by bulk electrons affects the location of the first energy minimum.

These conclusions are in agreement with our main result, Eq. (9). In particular, we note that the Fermi energy for Cu(111) is well within the quadratic regime;[30] Eq. (9) thus predicts that the interaction is isotropic, as seen in Fig. 2 of Ref. 7. We estimate also that the corresponding ratio $\epsilon_F/\epsilon \lesssim 1$, which suggests $\mathfrak{n}(\epsilon_F/\epsilon) < \mathcal{O}(1)$ (cf. Fig. 3). The far-field limit, defined as $R/\mathfrak{n}(\epsilon_F/\epsilon) \gg 1$, should be satisfied for Cu(111) at distances $R \gtrsim 10$ (at least ten atomic spacings), in agreement with the results of Ref. 7; corrections to Eq. (9) are $\mathcal{O}(R^{-1})$,

less than about 10% as large as the leading-order expression for the interaction.

C. The anisotropic interaction on Ag(111)

In Ref. 10, the SS-mediated adatom interaction is calculated in the far-field regime for an Ag(111) surface using DFT. Our analysis agrees with their results, insofar as Eq. (9) predicts a sixfold anisotropy in the interaction wavelength. However, Ref. 10 predicts that the wavelength may change by almost 50% as a function of θ. Comparing their numerics with our (one parameter) band structure suggests that $\epsilon_F/\epsilon < 0.5$ for strained Ag(111), so that Eq. (13) is a good approximation to Eq. (2), and Eq. (9) is well within the isotropic regime. Since the tight-binding ansatz might modestly underestimate the actual leading-order anisotropy, we considered the effect of enhancing this anisotropy by an order of magnitude; to more emphatically rule out the role of the leading-order anisotropy, we also examined the effect of enhancement by 2 and by 3 orders of magnitude. Our conclusion remains valid even when the anisotropy in Eq. (13) is increased by 10^3 (cf. Fig. 4). Thus, our analysis predicts negligible anisotropy in the adatom interaction on Ag.

Reference 10 also indicates that the amplitude of the interaction can decrease by as little as a factor of 2 over five or six atomic lengths; this does not agree with the $1/R^2$ envelope bounding oscillations in Eq. (9). Our analysis therefore implies that the SS-mediated RKKY interaction alone cannot account for the results found in Refs. 9 and 10.

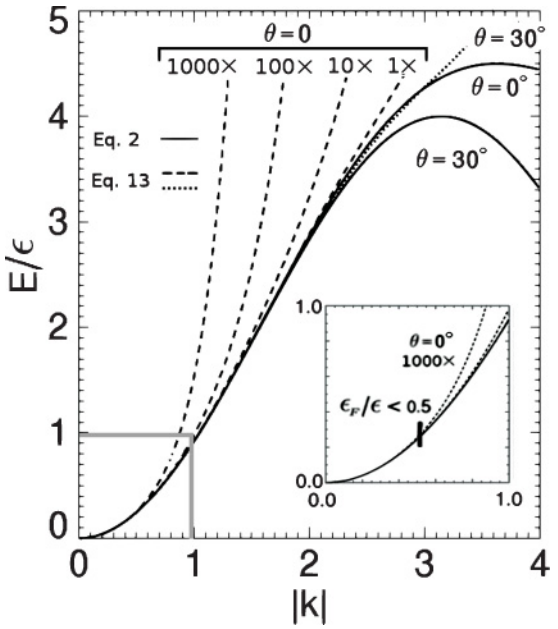

FIG. 4. Equations (2) and (13) as functions of k for $\theta = 0$ and $\theta = 30^\circ$. For Eq. (13), we also magnify the leading-order anisotropy, $[1 + \cos(6\theta)](a|\mathbf{k}|)^6/3240$, by factors of 10,100, and 1000. For $\epsilon_F/\epsilon < 0.5$ [corresponding to Ag(111)], the inset shows that even with a thousandfold enhancement, the leading-order anisotropy does not contribute significantly to the band structure in the vicinity of the Fermi energy. Consequently, our model predicts an *isotropic* RKKY interaction between adatoms on Ag(111).

Our model does not incorporate surface stress.[37] In Ag/Pt systems, lattice mismatch creates strain in the Ag layers, which, in principle, affects the band structure of the SS. References 9 and 10 included the effects of strain in their DFT calculations, which could account for discrepancies between Eq. (9) and their results. Furthermore, Eq. (1) neglects certain quantum-mechanical effects[17] (e.g., correlation energies) that are, in principle, incorporated into DFT; such effects could be responsible for the variation of the interaction found in Refs. 9 and 10.

D. Extensions to other systems

1. Key quantities determining the RKKY interaction

The steps leading to Eq. (9) can easily be generalized to systems having different band structures or indirect coupling modes. Our key approximation is that, in the far-field limit, Eq. (1) is dominated by the *local* behavior of the band structure at the points where the Fermi velocity is parallel or antiparallel to the adatom separation vector. This local behavior is contained explicitly in Eq. (6), and the implementation of our approximation comes when Eq. (5) is substituted into Eq. (3), rendering the subsequent integral (effectively) Gaussian.

To compute the anisotropic RKKY interaction for a different band structure, it is therefore sufficient to know only the second derivative (as a function of arc length) and the critical points of the constant-energy curves (in the vicinity of the Fermi contour) in a rotated frame in which $\mathbf{R}$ points in the $\hat{\mathbf{y}}$ direction (cf. Fig. 1). These derivatives may be calculated numerically when experimental data provides the best available representations of the SS band structure.

Our main result, Eq. (9), can also be applied to magnetically coupled systems (without spin-orbit coupling) since the exchange integral $|J_{\mathbf{kk}'}|^2$ can accommodate information about spin states.

2. Surface states at special points on the surface Brillouin zone edges

On the (110) faces of Cu, Ag, and Au, there is a metallic surface state centered at $\bar{Y}$, the middle of the longer edge of the rectangular surface Brillouin zone (SBZ).[38–40] There is no reason to expect that these SSs are isotropic; indeed, Simon *et al.*[40] calculate the semiminor and semimajor axes of the elliptical Fermi edge on Cu to be 1.38 and 1.64 nm^{-1}, respectively, with a ratio 0.84. In their computation of RKKY interactions in these principal directions, they find what amounts to $\pi/\lambda_F = 1.41$ and 1.72 nm^{-1}, respectively.

For the unusual[41] hcp metal beryllium, there are similar observations. On the close-packed, basal, (0001) face there is a nearly isotropic metallic surface state[42] centered at $\bar{\Gamma}$. On Be$(10\bar{1}0)$ there is a metallic surface state with its minimum at $\bar{A}$, the center of the longer edge of the rectangular surface Brillouin zone, with anisotropic (elliptical) constant-energy contours[43,44] and consequent anisotropy in the resulting RKKY interactions.[43] The Fermi ellipse is more eccentric than that of Cu(110), with an aspect ratio of about 0.71 (and semiaxes 2.2 and 3.1 nm^{-1}).[23] The ratio of the wavelengths of charge-density oscillations spawned by step edges in the two principal directions has a similar, though slightly higher, value

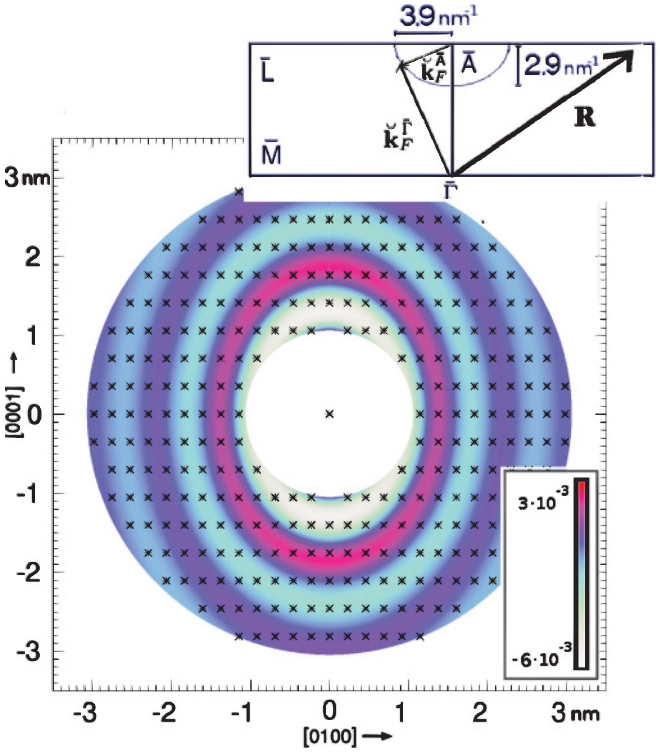

FIG. 5. (Color online) The normalized interaction energies $\mathcal{V}_F\Delta/(\pi^2|J_{\epsilon_F,\epsilon_F}|^2)$ for the elliptic Fermi edge of Be(10$\bar{1}$0) (shown, to scale, in the inset) drawn by choosing $\check{\mathbf{k}}_F = \check{\mathbf{k}}_F^{\bar{A}}$. Stars are Bravais lattice positions. The vector $\mathbf{k}_{\bar{A}} \equiv \frac{1}{2}\mathbf{G}_{\bar{\Gamma}\bar{A}\bar{\Gamma}}$ points from $\bar{\Gamma}$ to $\bar{A}$. In the inset, we show two choices of the spanning vector $\check{\mathbf{k}}_F$, viz., $\check{\mathbf{k}}_F^{\bar{A}}$ and $\check{\mathbf{k}}_F^{\bar{\Gamma}}$, and the corresponding separation vector $\mathbf{R}$. Note that $\check{\mathbf{k}}_F^{\bar{A}} = \check{\mathbf{k}}_F^{\bar{\Gamma}} - \mathbf{k}_{\bar{A}}$. In the main figure, we omit a circular region whose radius is roughly 1 nm since (i) the far-field approximation is not valid near the origin and (ii) the interaction energy diverges as $R \to 0$.

around 0.74. However, we are not aware of any data for the dependence of oscillations on steps with arbitrary azimuthal orientation that would allow comparison with our analysis. Charge-density oscillations were also observed around pointlike scatterers. The experiments noted the asymmetry of these contours.

Assuming an elliptical Fermi edge, we can apply Eq. (9b) to predict the azimuthal dependence of the RKKY interaction for Be(10$\bar{1}$0) as well as Cu(110). In Fig. 5 we carry out this task for Be(10$\bar{1}$0) by numerically computing $\mathfrak{n}(\epsilon_F)$ and $\check{\mathbf{k}}_F$. The plot shows interaction energy as a function of azimuthal orientation and distance from a central atom. The inset shows the upper half of the rectangular first surface Brillouin zone. Recalling the discussion after Eq. (1), we reemphasize that when comparing energies given by Eq. (9) and Fig. 5, care must be taken to ensure that $\mathbf{R}$ is a Bravais lattice vector.

We note that, as a consequence, the vector $\check{\mathbf{k}}_F$ underlying k_s in Eq. (9) is only determined modulo the addition of a reciprocal lattice vector. The crucial quantity in Eq. (9) is $\mathrm{sgn}[\mathcal{V}_\mathcal{F}]\,2\,k_s\,R = \mathrm{sgn}[\mathcal{V}_F]\,2\check{\mathbf{k}}_F \cdot \mathbf{R}$, where sgn is the signum function. The above product is invariant (modulo factors of 2π) under subtraction of a reciprocal lattice vector $\mathbf{G}$ from $2\check{\mathbf{k}}_F$ since any change of sign in $\check{\mathbf{k}}_F \cdot \mathbf{R}$ will be accompanied by a corresponding change of sign in $\mathcal{V}_F$ (see Fig. 5, for example). The two wave vectors $\check{\mathbf{k}}_F$ and $\check{\mathbf{k}}_F - \frac{1}{2}\mathbf{G}$ then correspond to different choices of the origin in $\mathbf{k}$ space.

In Fig. 5 we show two possible choices of $\check{\mathbf{k}}_F$ having $\bar{\Gamma}$ and $\bar{A}$ as their respective origins. When applying Eq. (9) to Be(10$\bar{1}$0), we can view the Fermi contour as a single contiguous ellipse with "inner" spanning vectors across it and energy gradients pointing outward, rather than (or as well as) a pair of semiellipses with "outer" spanning vectors across the SBZ and with inward-pointing (toward $\overline{\Gamma}$) gradients. We note that when used in conjunction with Eq. (9), different choices of $\check{\mathbf{k}}_F$ will result in different (and physically unmeaningful) *interpolations* of the interaction *between* Bravais lattice points.

E. Comparison to other analytical approaches

In Ref. 20 Hyldgaard and Persson calculate the SS-mediated adatom interaction using a technique based on the Harris energy functional.[45,46] Their approach yields a nonperturbative, analytic estimate of the indirect interaction that accounts for (i) a phase shift, which occurs when a SS scatters from an adatom, and (ii) damping of the interaction amplitude due to screening by bulk atoms.

While both of these effects are seen in some experimental systems,[20] we emphasize that they arise from *localized* aspects of adatom coupling to the SS and so do not affect the characteristic wavelength or decay of the interaction. Since our main task is to account for anisotropy in the adatom-*pair* interaction, we choose not to complicate our calculation with these effects to avoid clouding our discussion on the origin of anisotropy. Analytically, this choice was made when we set the exchange integral $|J_{\mathbf{k}\mathbf{k}'}|^2$ equal to a constant; as this term describes the detailed coupling between an adatom and surface state, its careful evaluation should yield information about the phase shift and screening.

F. Systems with complications not considered in the present analysis

For heavy metals, spin-orbit coupling plays a significant role in determining the SS band structure; for the present problem, it leads to splittings of SS bands, called Bychkov-Rashba splitting.[40,47] Perhaps the most widely known example is the metallic surface state on Au(111) at $\overline{\Gamma}$ in the L gap of the projected band states; a splitting of 0.25 nm^{-1}, with no detectable azimuthal dependence, is observed (viz., $k_F = 1.72$, 1.97 nm^{-1}).[48,49] Excellent agreement is obtained with fully relativistic DFT calculations,[49] while a simple tight-binding model[50] yields a splitting several orders of magnitude smaller than the relativistic calculations.[49] In fits of their calculations of the RKKY exchange interaction, Simon *et al.*[40] obtained good agreement with their calculated results by using the sum of two oscillatory curves with $k_F = 1.04$, 1.42 nm^{-1}.[51]

The distinctive[52] semimetal Bi displays the strongest reported spin-orbit splitting of surface bands, thrice that in Au, and considerable anisotropy.[53] Furthermore, theoretical analysis for Bi is more taxing: For Au(111) one can adequately describe the electronic dispersion by adding a Rashba term to the nonrelativistic Hamiltonian since the SS is free-electron-like and centered at $\overline{\Gamma}$; consequently, the splitting is linear in $\mathbf{k}$.[53] For Bi, the surface states are not free-electron-like and are distributed over the surface Brillouin zone; hence,

first-principles relativistic band structure methods are needed to model the complex behavior SS dispersion.[53] For the (111) surface there are six elongated hole pockets along $\overline{\Gamma M}$ surrounding a ring-shaped electron pocket centered at $\overline{\Gamma}$, all with 2D character.[53,54] Spin-orbit coupling not only decreases the size of the Fermi surface hexagon by 30% but also introduces hole lobes and turns the SS into a surface resonance. On the (110) surface there is a hole metallic surface band centered at $\overline{\Gamma}$, and only one branch of the split state can be observed.[53,55] On the (001) surface, there is a hexagonal electron pocket around $\overline{\Gamma}$ and six hole lobes along the $\overline{\Gamma}$-$\bar{M}$ directions as well as indication of an electron pocket around $\bar{M}$.[52,53,56]

When considering exchange coupling between magnetic adatoms, spin-orbit coupling introduces another complication: the exchange coupling can lead to canting of the two spins in a coupled pair,[57] which often must be neglected to make calculations feasible.[58]

Another complication is that surface states can produce surface relaxation.[59] In particular, unusually large inward relaxations were noted on Cu(110)[60] and Be($10\bar{1}0$).[61] Lateral relaxations due to perturbations are known to complicate the description of lattice gases in terms of adsorbate interactions.[62]

In graphene all one-electron states are *ipso facto* 2D states. Not surprisingly, then, many theory groups have recently devoted attention to the prospect of RKKY interactions.[63–74] They and others pointed out a variety of complicating issues and idiosyncrasies of monolayer graphene, such as the bipartite nature of the lattice (leading to ferromagnetic or repulsive coupling for impurities on the same hexagonal, Bravais sublattice of the honeycomb graphene lattice[63,64] and antiferromagnetic or attractive coupling when on opposite Bravais sublattices[64,65,68,69]), the vanishing density of states at the Fermi level in undoped and ungated lattices, the suppression of backscattering (leading to R^{-3} rather than R^{-2} decay[75]),[63,64] the role of electron-electron interactions,[70] etc. Usually, the adsorbates are taken in atop sites but sometimes in bridge sites above bonds or hollow sites at the center of the hexagon.[63,71] Since the Dirac cones are circularly symmetric, our analysis suggests that there should not be anisotropy in the RKKY interaction, but this neglects the chiral nature of the electrons: sizable threefold anisotropy is observed, which is typically attributed to intervalley scattering.[67,71] Hence, more detailed discussion of graphene is inappropriate here and distracting from the theme of this paper. Furthermore, actually observing the asymptotic oscillatory behavior typifying RKKY will generally pose a great challenge unless the graphene is heavily doped.

In topological insulators, a combination of spin-orbit coupling and time-reversal symmetry leads to protected metallic surface states.[76] Thus, RKKY interactions can be expected to play an important role. Examples of very recent studies are Refs. 77, 78, and 79.

G. Open directions

Our analysis could, in principle, be extended to treat trio (three-adatom nonpairwise) interactions.[24,80] Such interactions typically decay asymptotically as $d^{5/2}$, where d is the perimeter of the triangle made by the three interacting adatoms.[81] While any particular trio interaction is expected to be weaker than the three associated pair interactions, the difference in the decay envelope is just a half power (5/2 vs 2) for SS mediation. More significantly, the multiplicity of trios is greater; hence, trio interactions could still play a prominent role in the ordering of surface structures. The resulting extension of Eq. (9) would, in general, contain three different wavelengths and would be cumbersome to apply. This analysis is beyond the scope of the present study. We also note that multisite nonpairwise interactions between four or more adatoms could come into play, with even greater multiplicities and modest increases in the decay envelope. Checking how such a series converges to the energy of an ordered fractional overlayer was a challenge never fully met for rapidly decaying ($\propto R^{-5}$) interactions mediated by bulk states.[82] For an overlayer determined by surface-state-mediated interactions, with density so sparse that asymptotic interactions determine the ground state, verifying convergence would present a truly daunting task.

IV. CONCLUSION

In this paper, we derive an analytic formula for the surface-state-mediated RKKY interaction between adatoms. The main contribution to the interaction comes from surface states whose Fermi velocity is parallel to the vector connecting the adatoms. The interaction is oscillatory and has an envelope that falls off as $1/R^2$ (but eventually transitioning, at finite temperature, to exponential decay at distances larger than germane to this problem), in agreement with experimental results for Cu(111).[7,8] The amplitude and frequency of the interaction are anisotropic; they depend on the surface-state dispersion relation. Comparison with Refs. 9 and 10 indicates that the RKKY interaction alone, at least to the extent that the SS dispersion is adequately described by the tight-binding model, cannot be responsible for the anisotropy in the interaction between Ag adatoms adsorbed on Pt(111). Our work suggests that analytic treatment of other quantum-mechanical interactions (e.g., arising from correlations) and/or strain-induced effects in the SS band structure may be necessary to account for this anisotropy. We also show how our analysis can be applied to other systems such as Be($10\bar{1}0$) and discuss extensions of our work to multiadatom interactions.

ACKNOWLEDGMENTS

This work was supported by the NSF MRSEC under Grant No. DMR 05-20471 at the University of Maryland, with ancillary support from CNAM. Support for P.P. was also provided by the National Institute of Standards and Technology American Recovery and Reinvestment Act Measurement Science and Engineering Fellowship Program Award No. 70NANB10H026 through the University of Maryland. T.L.E. was secondarily supported by NSF Grant No. CHE-07-50334. The authors also wish to thank Dionisios Margetis, Gregg Gallatin, and Mark Stiles for useful comments and discussion during preparation of this paper. T.L.E. acknowledges fruitful collaboration with Per Hyldgaard and, more recently, Kristian Berland on related problems.

*ppatrone@umd.edu
†einstein@umd.edu

[1] J. Frenkel and T. Kontorova, J. Phys. (USSR) **1**, 137 (1939).
[2] P. Bak, Rep. Prog. Phys. **45**, 587 (1982).
[3] S. Narasimhan and D. Vanderbilt, Phys. Rev. Lett. **69**, 1564 (1992).
[4] J. C. Hamilton, Phys. Rev. Lett. **88**, 126101 (2002).
[5] J. C. Hamilton and S. M. Foiles, Phys. Rev. Lett. **75**, 882 (1995).
[6] R. Pushpa, J. Rodriguez-Laguna, and S. N. Santalla, Phys. Rev. B **79**, 085409 (2009).
[7] V. S. Stepanyuk, A. N. Baranov, D. V. Tsivlin, W. Hergert, P. Bruno, N. Knorr, M. A. Schneider, and K. Kern, Phys. Rev. B **68**, 205410 (2003).
[8] V. S. Stepanyuk, L. Niebergall, R. C. Longo, W. Hergert, and P. Bruno, Phys. Rev. B **70**, 075414 (2004).
[9] J. D. Howe, P. Bhopale, Y. Tiwary, and K. A. Fichthorn, Phys. Rev. B **81**, 121410(R) (2010).
[10] W. Luo and K. A. Fichthorn, Phys. Rev. B **72**, 115433 (2005).
[11] H. Brune, H. Roder, C. Boragno, and K. Kern, Phys. Rev. B **49**, 2997 (1994).
[12] S. G. Davison and M. Stęślicka, *Basic Theory of Surface States* (Oxford University Press, Oxford, 1996).
[13] P. Han and P. S. Weiss, Surf. Sci. Rep. **67**, 19 (2012).
[14] M. A. Ruderman and C. Kittel, Phys. Rev. **96**, 99 (1954).
[15] K. Yosida, Phys. Rev. **106**, 893 (1959).
[16] T. Kasuya, Prog. Theor. Phys. **16**, 45 (1956).
[17] C. Kittel, Solid State Phys. **22**, 1 (1968).
[18] K. H. Lau and W. Kohn, Surf. Sci. **75**, 69 (1978).
[19] B. Fischer and M. W. Klein, Phys. Rev. B **11**, 2025 (1975); M. T. Béal-Monod, *ibid.* **36**, 8835 (1987).
[20] P. Hyldgaard and M. Persson, J. Phys. Condens. Matter **12**, L13 (2000).
[21] For the (100) surface, considerable analytical progress on constituent Green's functions can be made before performing asymptotic approximations; G. D. Mahan, Int. J. Mod. Phys. B **9**, 1327 (1995); See also T. L. Einstein, Surf. Sci. **75**, L161 (1978). We have not been able to generalize this approach to the geometry of the (111) case and so adopt an approach in the tradition of Lau and Kohn; see Ref. 18, for example.
[22] In studying the oscillatory exchange coupling of magnetic multilayers, F. Herman and R. Schrieffer [Phys. Rev. B **46**, 5806 (1992)] showed that long-period superoscillations in the RKKY coupling could be explained by generalizing plane-wave wave functions to Bloch functions as well as incorporating boundary scattering at the film edges. The latter effect is irrelevant here, and we do not complicate our analysis with the former, given that there is no evidence for analogous superoscillations in adatom-adatom interactions.
[23] B. G. Briner, P. Hofmann, M. Doering, H.-P. Rust, E. W. Plummer, and A. M. Bradshaw, Phys. Rev. B **58**, 13931 (1998).
[24] T. L. Einstein, in *Physical Structure of Solid Surfaces*, edited by W. N. Unertl (Elsevier, Amsterdam, 1996), Chap 11.
[25] L. M. Roth, H. J. Zeiger, and T. A. Kaplan, Phys. Rev. **149**, 519 (1966).
[26] S. Lounis, P. Zahn, A. Weismann, M. Wenderoth, R. G. Ulbrich, I. Mertig, P. H. Dederichs, and S. Blügel [Phys. Rev. B **83**, 035427 (2011)] very recently revisited with greater detail and novel applications the RKKY for anisotropic Fermi surfaces in 3D.
[27] At $\overline{\Gamma}$ there is also a deeper, filled SS as well as a higher, empty image-potential SS. For example, for Cu(111) photoemission finds the minimum of the former at −5.25 eV [S. G. Louie, P. Thiry, R. Pinchaux, Y. Pétroff, D. Chandesris, and J. Lecante, Phys. Rev. Lett. **44**, 549 (1980); S. D. Kevan, N. G. Stoffel, and N. V. Smith, Phys. Rev. B **31**, 3348 (1985)], while inverse photoemission finds the minimum of the latter several eV above E_F [W. Jacob, V. Dose, U. Kolac, Th. Fauster, and A. Goldmann, Z. Phys. B **63**, 459 (1986)].
[28] S. D. Kevan and R. H. Gaylord, Phys. Rev. B **36**, 5809 (1987).
[29] L. Bürgi, L. Peterson, H. Brune, and K. Kern, Surf. Sci. Lett. **447**, L157 (2000).
[30] K. Berland, T. L. Einstein, and P. Hyldgaard, Phys. Rev. B **85**, 035427 (2012).
[31] This substitution maps the lower integration domain ($k_y < 0$) onto the upper domain ($k_y > 0$). All information about the lower integration domain is then contained in Eq. (4).
[32] The $k_x(k_x')$ limits of integration are functions of $E(E')$ in Eq. (3), and $k_y = k_y(E,k_x)$ in Eq. (4). Recall that the group velocity of a wave packet is the gradient of the dispersion relation.
[33] For justification, see, for example, C. M. Bender and S. Orszag, *Advanced Mathematical Methods for Scientists and Engineers* (Springer, New York, 1999), pp. 276–279.
[34] Following Ref. 25, we assume that $J_{\mathbf{k}\mathbf{k}'}$ is a slowly varying function of $\mathbf{k}$ and $\mathbf{k}'$.
[35] In this context, the expression $g = \mathcal{O}(\delta)$ signifies that g/δ is bounded by constant as $\delta \to 0$.
[36] Calculations of a similar nature were performed for Co adsorbates on Pt(111) 58, for which the Shockley state is empty, and for Co and Fe on the principal faces of Cu and Au 40. In the latter, interactions were computed out to at least 20 neighbor spacings, but there is no discussion of anisotropy for the (111) faces.
[37] Our model also does not include spin-orbit coupling for Ag(111) since it is not seen experimentally. From theory, a splitting of 0.013 nm^{-1} is expected, an order of magnitude below the experimental angular resolution, as discussed in Ref. 49.
[38] Similarly, there is evidence of a more fragile metallic surface state on noble-metal surfaces at the $\bar{Y}$ point [W. W. Pai, J. S. Ozcomert, N. C. Bartelt, T. L. Einstein, and J. E. Reutt-Robey, Surf. Sci. **307–309**, 747 (1994); S. H. Liu, C. Hinnen, C. N. van Huong, N. R. de Tacconi, and K.-M. Ho, J. Electroanal. Chem. **176**, 325 (1984); R. Courths, H. Wern, U. Hau, B. Cord, V. Bachelier, and S. Hüfner, J. Phys. F **14**, 1559 (1984)]. Note also the 2D RKKY-like behavior found in calculations of interactions between Co atoms on the (110) faces of noble metals [E. Simon, B. Lazarovits, L. Szunyogh, and B. Újfalussy, Philos. Mag. **88**, 2667 (2008)].
[39] L. Petersen, B. Schaefer, E. Lægsgaard, I. Stensgaard, and F. Besenbacher, Surf. Sci. **457**, 319 (2000).
[40] E. Simon, B. Újfalussy, B. Lazarovits, A. Szilva, L. Szunyogh, and G. M. Stocks, Phys. Rev. B **83**, 224416 (2011).
[41] E. W. Plummer and J. B. Hannon, Prog. Surf. Sci. **46**, 149 (1994).
[42] P. T. Sprunger, L. Petersen, E. W. Plummer, E. Læsgaard, and F. Besenbacher, Science **275**, 1764 (1997).
[43] Ph. Hofmann, B. G. Briner, M. Doering, H.-P. Rust, E. W. Plummer, and A. M. Bradshaw, Phys. Rev. Lett. **79**, 265 (1997).
[44] T. Balasubramanian, L. I. Johansson, P.-A. Glans, C. Virojanadara, V. M. Silkin, E. V. Chulkov, and P. M. Echenique, Phys. Rev. B **64**, 205401 (2001).

[45]P. Hyldgaard and M. Persson, Chalmers/Göteborg University, Appl. Phys. Rep. No. 1999-36, 1999 (unpublished).
[46]J. Harris, Phys. Rev. B **31**, 1770 (1985).
[47]Yu. A. Bychkov and E. I. Rashba, JETP Lett. **39**, 78 (1984).
[48]S. LaShell, B. A. McDougall, and E. Jensen, Phys. Rev. Lett. **77**, 3419 (1996).
[49]G. Nicolay, F. Reinert, S. Hüfner, and P. Blaha, Phys. Rev. B **65**, 033407 (2001).
[50]L. Petersen and P. Hedegård, Surf. Sci. **459**, 49 (2000).
[51]Simon *et al.* attribute their smaller values of k_F to the imprecise treatment of the surface potential in their calculational scheme.
[52]T. Hirahara, T. Nagao, I. Matsuda, G. Bihlmayer, E. V. Chulkov, Yu. M. Koroteev, P. M. Echenique, M. Saito, and S. Hasegawa, Phys. Rev. Lett. **97**, 146803 (2006).
[53]Yu. M. Koroteev, G. Bihlmayer, J. E. Gayone, E. V. Chulkov, S. Blügel, P. M. Echenique, and Ph. Hofmann, Phys. Rev. Lett. **93**, 046403 (2004).
[54]C. R. Ast and H. Höchst, Phys. Rev. Lett. **87**, 177602 (2001).
[55]S. Agergaard, Ch. Søndergaard, H. Li, M. B. Nielsen, S. V. Hoffmann, Z. Li, and Ph. Hofmann, New J. Phys. **3**, 15 (2001).
[56]T. Hirahara, K. Miyamoto, I. Matsuda, T. Kadono, A. Kimura, T. Nagao, G. Bihlmayer, E. V. Chulkov, S. Qiao, K. Shimada, H. Namatame, M. Taniguchi, and S. Hasegawa, Phys. Rev. B **76**, 153305 (2007).
[57]M. Bode, M. Heide, K. von Bergmann, P. Ferriani, S. Heinze, G. Bihlmayer, A. Kubetzka, O. Pietzsch, S. Blügel, and R. Wiesendanger, Nature (London) **447**, 190 (2007).
[58]L. Zhou, J. Wiebe, S. Lounis, E. Vedmedenko, F. Meier, S. Blügel, P. H. Dederichs, and R. Wiesendanger, Nat. Phys. **6**, 187 (2010). In earlier work members of this group [J. Wiebe, F. Meier, K. Hashimoto, G. Bihlmayer, S. Blügel, P. Ferriani, S. Heinze, and R. Wiesendanger, Phys. Rev. B **72**, 193406 (2005)] found that on clean Pt(111) the Shockley state is unoccupied (nonmetallic) but that some bulk bands contribute strongly to the local density of states at the surface. Zhou *et al.* find strong directional dependence in the RKKY interaction and can fit to the generic 2D expression in the close-packed $[1\bar{1}0]$ direction.
[59]V. Chis and B. Hellsing, Phys. Rev. Lett. **93**, 226103 (2004).
[60]Y.-P. Xie, Y. Luo, and S.-J. Liu, Chin. Phys. **16**, 1429 (2007).
[61]S.-J. Tang, H.-T. Jeng, C.-S. Hsue, Ismail, P. T. Sprunger, and E. W. Plummer, Phys. Rev. B **77**, 045405 (2008).
[62]R. Sathiyanarayanan, T. J. Stasevich, and T. L. Einstein, Surf. Sci. **602**, 1243 (2008); R. Sathiyanarayanan and T. L. Einstein, *ibid.* **603**, 2387 (2009).
[63]V. V. Cheianov and V. I. Fal'ko, Phys. Rev. Lett. **97**, 226801 (2006); V. V. Cheianov, Eur. Phys. J. Spec. Top. **148**, 55 (2007); V. V. Cheianov, V. Fal'ko, O. Syljuåsen, and B. L. Altshuler, Solid State Commun. **149**, 1499 (2009); V. V. Cheianov, O. Syljuåsen, B. L. Altshuler, and V. Fal'ko, Phys. Rev. B **80**, 233409 (2009); Europhys. Lett. **89**, 56003 (2010).
[64]L. Brey, H. A. Fertig, and S. Das Sarma, Phys. Rev. Lett. **99**, 116802 (2007); E. H. Hwang and S. Das Sarma, *ibid.* **101**, 156802 (2008).
[65]S. Saremi, Phys. Rev. B **76**, 184430 (2007).
[66]C. Bena and S. A. Kivelson, Phys. Rev. B **72**, 125432 (2005); C. Bena, Phys. Rev. Lett. **100**, 076601 (2008).
[67]L. Simon, C. Bena, F. Vonau, D. Aubel, H. Nasrallah, M. Habar, and J. C. Peruchetti, Eur. Phys. J. B **69**, 351 (2009).
[68]J. E. Bunder and H.-H. Lin, Phys. Rev. B **80**, 153414 (2009).
[69]A. V. Shytov, D. A. Abanin, and L. S. Levitov, Phys. Rev. Lett. **103**, 016806 (2009); D. A. Abanin, A. V. Shytov, and L. S. Levitov, *ibid.* **105**, 086802 (2010).
[70]A. M. Black-Schaffer, Phys. Rev. B **82**, 073409 (2010).
[71]M. Sherafati and S. Satpathy, Phys. Rev. B **83**, 165425 (2011); **84**, 125416 (2011).
[72]B. Uchoa, T. G. Rappoport, and A. H. Castro Neto, Phys. Rev. Lett. **106**, 016801 (2011); **106**, 159901(E) (2011).
[73]E. Kogan, Phys. Rev. B **84**, 115119 (2011).
[74]Section IV G of A. H. Castro Neto, F. Guinea, N. M. R. Peres, K. S. Novoselov, and A. K. Geim [Rev. Mod. Phys. **81**, 109 (2009)] has a short review of RKKY in graphene.
[75]For doped graphene, with nonvanishing k_F, the leading-order R^{-2} interaction still vanishes due to cancellations between the same and opposite sublattices, leaving again R^{-3} decay. For undoped graphene, with vanishing k_F, the amplitude of the R^{-3} decay is very large. For doped or gated bilayer graphene the familiar 2D behavior is seen, with R^{-2} oscillatory asymptotic decay (Ref. 64). Reference 69 also discusses R^{-1} decay.
[76]M. Z. Hasan and C. L. Kane, Rev. Mod. Phys. **82**, 3045 (2010).
[77]Q. Liu, C.-X. Liu, C. Xu, X.-L. Qi, and S.-C. Zhang, Phys. Rev. Lett. **102**, 156603 (2009).
[78]D. A. Abanin and D. A. Pesin, Phys. Rev. Lett. **106**, 136802 (2011).
[79]J.-J. Zhu, D.-X. Yao, S.-C. Zhang, and K. Chang, Phys. Rev. Lett. **106**, 097201 (2011).
[80]T. L. Einstein, Langmuir **7**, 2520 (1991).
[81]P. Hyldgaard and T. L. Einstein, Europhys. Lett. **59**, 265 (2002); J. Cryst. Growth **275**, e1637 (2005).
[82]T. L. Einstein, Phys. Rev. B **16**, 3411 (1977).